



Numerical and Performance Analysis of a Hybrid Savonius–Darrieus Vertical Axis Wind Turbine with Leaf-Shaped Blades

Lina Jassim^{1*}, Nibras M. Mahdi², Jasmine Aziz Hussein³, Muhammad Asmail Elewi⁴, Hasan Shakir Majdi⁵

¹ Mechanical Engineering Department, Mustansiriyah University, Baghdad 10052, Iraq

² Mechanical Engineering College, University of Technology - Iraq, Baghdad 10066, Iraq

³ Continuing Education Unit, College of Engineering, Al- Iraqia University, Baghdad 10053, Iraq

⁴ Electromechanical Engineering Department, College of Engineering, University of Samarra, Samarra 34010, Iraq

⁵ Department of Chemical Engineering and Petroleum Industries, Al-Mustaqbal University College, Hillah 51001, Iraq

Corresponding Author Email: dr.linajassim@uomustansiriyah.edu.iq

Copyright: ©2026 The authors. This article is published by IETA and is licensed under the CC BY 4.0 license (<http://creativecommons.org/licenses/by/4.0/>).

<https://doi.org/10.18280/ijht.440130>

ABSTRACT

Received: 18 October 2025

Revised: 17 January 2026

Accepted: 27 January 2026

Available online: 28 February 2026

Keywords:

hybrid vertical axis wind turbine, Savonius and Darrieus rotor, leaf-shaped blade, multi-stage turbine, torque and power output, electrical efficiency, computational fluid dynamics simulation, wind energy in urban areas

This work describes the design, model, and performance analysis of a hybrid leaf-shaped vertical axis wind turbine (VAWT) that utilizes the drag-driven Savonius and lift-driven Darrieus to maximize energy conversion efficiency. Standard single-stage three-blade Darrieus, compared to hybrid, 2- and 3-stage turbines with three, four, and five blades per stage, was tested. Mechanical analysis was performed with momentum-based modeling and computational fluid dynamics (CFD) simulation, and electrical performance calculation through generator–rectifier simulation under wind conditions similar to the conditions of Baghdad. The baseline turbine produced the highest overall efficiencies but the lowest torque and power — the torque was 13.6 N·m, the power 237 W, and the efficiencies, mechanically 0.342 and electrically 0.737 at 20 m hub height. The 2-stage × 3-blade turbine, in comparison, gave 23.4 N·m torque and 294 W, but mechanical efficiency decreased to 0.212. The 3-stage × 3-blade turbine displayed the highest performance, providing 34.3 N·m and 416 W on a 20 m rotation, and 60.5 N·m during the 100 m rotation speed — electrically producing up to 7.78 A, 747 W for 0.782 efficiency, surpassing all other combinations. Increase the blade number in the stage to four and five so as to increase blade pressure too (13.5 Pa), but reduce efficiency because of aerodynamic drag. The research proves that turbine height and stage number are the principal elements affecting performance; however, too many blades result in efficiency losses. The 3-stage × 3-blade hybrid turbine was established as the optimal layout and has the best trade ratio between torque, electrical yield, and efficiency, which can be useful in decentralized wind energy harvesting in urban areas such as Baghdad.

1. INTRODUCTION

A trend of increasing global demand for clean and renewable energy sources has led to increased research that is focused on the application of wind energy technologies, and vertical axis wind turbines (VAWTs) specifically, which are a good candidate for urban and low wind speed applications given their omnidirectional wind acceptance, minimal noise, and simple maintenance. Conventional VAWTs, however, come with performance limitations, such as poor self-starting capability in Darrieus turbines and low efficiency in Savonius turbines. Hybrid VAWT configurations exploiting Savonius and Darrieus rotors have been suggested due to the high starting torque of Savonius and the superior aerodynamic efficiency of Darrieus. In this study, the advanced bio-inspired hybrid leaf-shaped blade VAWT is designed for improved aerodynamic performance and self-starting capabilities. Its leaf shapes not only improve flow interaction but also reduce turbulence and increase power generation. It is assessed based

on computational fluid dynamics (CFD) simulations and experimental tests, and compared to an existing hybrid VAWT. The results demonstrate the potential of this proposed turbine as a scalable and efficient solution for decentralized wind energy generation in low- to moderate-wind urban environments.

Arrieta-Gomez et al. [1] designed a regression-based optimization framework together with CFD for hybrid Savonius–Darrieus hydrokinetic turbines to improve performance. Due to their experiment design, they obtained excellent performance improvements, demonstrating the need for parametric optimization for hybrid systems. Charlesantonyraj et al. [2] presented a butterfly-inspired vertical axis wind plant for enhancing aerodynamic activities in urban. They indicated, among other things, that bio-inspired blade geometry may improve lift properties and, in general, turbine efficacy. Chaudhuri et al. [3] reviewed multiple energy conversion strategies for wind energy systems from electrical, mechanical, and material aspects. This study focuses on the

integration of multidisciplinary approaches to improve overall system performance and durability. Dewan et al. [4], we outlined the trends in Savonius wind turbine design and performance techniques that have been studied closely to date. They discovered alterations to blade form customization and flow controllers for greater efficiency. Fertahi et al. [5] studied a hybrid tidal turbine combining Savonius and Darrieus rotors using CFD analysis. The study found that nested hybridization, based on the combination of hybridized flow rates of the two rotors, dramatically increases starting torque and operating efficiency at low flow velocities. Eftekhari et al. [6] performed a numerical study in a hybrid Savonius–Darrieus turbine under low-wind speeds in a grid of turbines for the first time as part of a series of simulations on a numerical hybrid Savonius–Darrieus turbine. They further corroborated their results, demonstrating the enhanced self-starter capability and superior aerodynamics among the single or two-rotor configurations. Eltayesh et al. [7] compared aerodynamic improvements in Darrieus VAWTs with blade changes. The analysis results demonstrated significant enhancements in power coefficient and flow stability over wind modes. Fazylova et al. [8] conducted a comparative analysis on Savonius turbines and Darrieus turbines by examining their design and operation aspects. Hybrid configurations combine the benefits of both systems for performance with some degree of synergy. In this regard, a dual-shaft configuration proposed by Ghafoorian et al. [9] has advanced self-starting capability of hybrid turbines. They obtained improved efficiency and torque production when compared to a conventional single shaft. Ghafoorian et al. [10] looked into the use of a curtain for enhancing the aerodynamic behavior of a hybrid turbine. The results indicate that flow control greatly improves energy acquisition while also limiting aerodynamic losses. Consequently, Gupta and Biswas [11] conducted a CFD analysis of a joint Savonius–Darrieus turbine for flow physics, in addition to an integrated wind turbine for the model development of flow physics. Their findings demonstrated that the drag-lift combination is beneficial for enhancing the turbine performance. Inácio et al. [12] used numerical simulations to study hybrid turbines in turbulent airflow applications under turbulent airflow in hybrid turbines using numerical simulations. We found that turbulence intensity strongly influences power output and aerodynamic efficiency in turbulence effects during the tests. The turbines developed for tidal energy applications on Darrieus–Savonius for tidal power were evaluated under the specificities of Kyoizuka's [13] experimental. A high-tidal power-extraction and aero-drilling methodology will be studied on the Darrieus–Savonius turbines. This study validated the applicability of hybrid designs for low-speed water currents, with better start characteristics. Lajnef et al. [14] studied the function, performance, and efficiency of helical Savonius rotors. What they found was that when compared with helical designs increases torque flow and power output. Liang et al. [15] compared the performance of the various torques of the hybrid turbine by radius ratio, as well as attachment angle, and found their relationship in two cases, by computationally analyzing these parameters. Optimal geometric parameters to maximize efficiency were identified in the study. Łyskawiński et al. [16] empirically studied vertical axis turbines for energy harvesting of passing vehicles. Their findings showed that hybrid designs can accommodate low, intermittent wind generators. Mohamed et al. [17] proposed a hybrid renewable energy system and wind turbines as an integrated renewable energy

system (hybrid windy wind in homes) to promote energy efficiency and sustainability for residential power supply. The contribution of hybrid turbines in improving system reliability and efficiency was stressed. Pallotta et al. [18] also presented a Hybrid Turbine Research Facility (HYBRI), which integrates Savonius and Darrieus rotors and investigates flow field characteristics. Their results demonstrated superior performance compared to their standalone turbine configurations. Pan et al. [19] presented a performance analysis of an idealized hybrid turbine based on advanced aerodynamic modeling. The synergistic effect of the combined lift and drag-based mechanism was proven in the study. A hybrid turbine's performance under varying operating conditions was numerically studied by Pouransari and Behzad [20]. Their findings presented better power coefficients and self-starting ability. Rathore et al. [21] proposed an aero-leaf Savonius turbine based on natural templates. The results indicate that bio-inspired approaches can vastly improve aerodynamic performance and environmental protection. Redchys et al. [22] performed a comparative study of single and combined rotor configurations in vertical-axis wind turbines. Hybrid systems significantly outclass single configurations in efficiency and performance. Sahim et al. [23] experimentally examined the hybrid turbine performance as a function of a deflector. Through well-directed airflow as well, deflectors were found to increase power output remarkably. Sahim et al. [24] reviewed the influence of rotor radius on hybrid turbine performance. The importance of engineering optimisation in terms of their work is highlighted there. The aerodynamic response of natural leaves against wind conditions was investigated by Vogel [25]. It shed light on bio-inspired schemes for enhancing turbine blade efficiency.

Previous research is classified as Savonius enhancement, hybrid designs, blade geometry, bio-inspired concepts, and multi-stage turbines. Consequences, limitations, and implications of the present work are addressed explicitly.

Though basic VAWT principles were set out in the early studies (2006–2014), recent developments have focused on CFD-based optimization and bio-inspired designs. Current research primarily considers efficiency enhancement, wake mitigation, and urban wind adaptability. These patterns are the impetus behind the system-level view taken up in the current study.

Hybrid VAWTs are still associated with a strong torque–efficiency trade-off caused by drag and flow separation, being highly inefficient. Designs of more classical blades are also common, but are unsuitable for low Reynolds number urban winds. Moreover, few are focusing on multi-stage configurations and coupled electro-mechanical behaviour.

A leaf-shaped blade in combination with a multi-stage hybrid VAWT architecture. The blade is effective for preventing flow separation and stall during low wind speed, with a multi-stage structure that enables the extraction of torque and the utilization of wind shear. An extensive CFD-mechanical-electrical analysis proves its utility for urban wind energy applications.

2. METHODOLOGY

The performance of a hybrid VAWT with leaf-shaped blades is a subject of the study of both electrical and numerical modeling in this paper. The approach is formulated in three basic stages, which are aerodynamic simulation, mechanical

performance evaluation, and electrical system modeling. Each step is destined to isolate the effect of blade number, turbine staging, and the height of installation on the total energy conversion process.

2.1 Turbine design

The hybrid VAWT that was developed employs a bio-inspired leaf-shaped rotor based on the principles of Savonius and Darrieus, for self-starting features and improved aerodynamic performance in rising wind speeds. The curvature and thickness-to-chord ratio of the blade were designed to minimize flow separation without sacrificing structural behavior. The ANSYS Fluent algorithm numerically examined various configurations with many different blade counts and stage numbers and determined that higher blade counts led to larger torque, with three-blade designs resulting in cleaner wakes and better efficiency. In general, the 3-stage \times 3-blade arrangement achieved the best balance between torque, power output, and efficiency under a wide range of wind conditions. Figure 1 shows the design of the turbine.

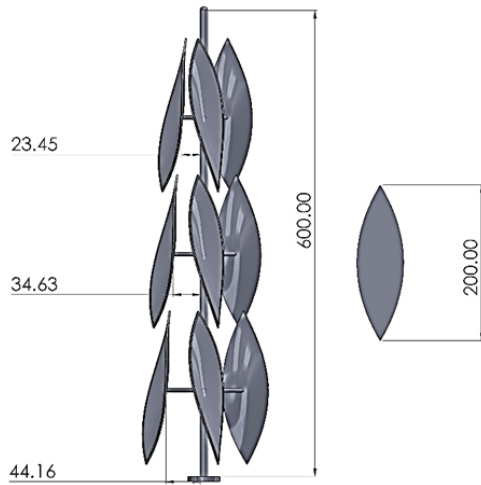


Figure 1. Design turbine

It is noteworthy to explain a performance benefit of the proposed leaf-shaped blade does not occur due to an overall aerodynamic advantage over other conventional airfoils like the NACA series but, instead, it is due to its practical applicability in hybrid, low-Reynolds-number, and multi-stage VAWT applications. As has been demonstrated by many studies, although symmetric NACA airfoils (e.g., NACA 00150021) work well in lift-dominated Darrieus rotors with higher tip speed ratios, they do not work well in low Reynolds number and strongly unsteady inflow environments characteristic of urban wind settings. Contrary, it has been documented that bio-inspired and non-conventional blade profiles developed smoother pressure gradients, slower flow separation, and better torque generation at lower tip speed ratios. Notably, the better performance enhancement of the leaf shape blade described here is not primarily due to higher aerodynamic efficiency than that of typical NACA airfoils, but rather to its suitability for hybrid and low-Reynolds-number VAWT purposes. Previous research like Rathore et al. [21] and Lajnef et al. [14], showed that in low tip speed ratios, bio-inspired and modified geometric configurations enhance the flow attachment and torque-generating performance. Furthermore, Ghafoorian et al. [9] pointed out that hybrid

configurations improved drag–lift interactions under unsteady flows and made it possible to utilize non-conventional blade designs for urban wind environments.

2.2 Governing equations and aerodynamic modeling

The mechanical performance was assessed using a momentum-based aerodynamic model complemented by CFD analysis in ANSYS Fluent (R19.0). The governing equations included the conservation of mass, momentum, and energy for incompressible turbulent flow:

- Continuity equation:

$$\nabla \cdot \vec{V} = 0 \quad (1)$$

- Momentum equation (Navier-Stokes):

$$\rho \left(\frac{\partial \vec{V}}{\partial t} + \vec{V} \cdot \nabla \vec{V} \right) = -\nabla p + \mu \nabla^2 \vec{V} \quad (2)$$

Here, \vec{V} is the velocity vector, ρ the air density, p the pressure, and μ the dynamic viscosity.

Torque (T) was calculated from blade aerodynamic forces as:

$$T = \sum (F_t \cdot r) \quad (3)$$

where, F_t is the tangential force on the blades and r is the rotor radius.

Mechanical power was obtained as:

$$P_{mech} = T \cdot \omega \quad (4)$$

where, ω is the angular velocity of the turbine. Mechanical efficiency was expressed as:

$$\eta_{mech} = \frac{P_{mech}}{P_{wind}}, P_{wind} = \frac{1}{2} \rho A V^3 \quad (5)$$

with A being the swept area and V the incoming wind velocity.

2.3 Wind profile with height

The variation of wind velocity with turbine height was modeled using the power-law profile:

$$V(z) = V_{ref} \left(\frac{z}{z_{ref}} \right)^\alpha \quad (6)$$

where, V_{ref} is the reference wind speed at height z_{ref} , and α is the wind shear exponent. For Baghdad conditions, $\alpha = 0.18$ was adopted, reflecting urban terrain effects. Simulations were conducted for three characteristic hub heights: 20 m, 50 m, and 100 m.

2.4 Electrical modeling

The electrical subsystem was modeled by coupling the turbine's mechanical shaft power to a generator-rectifier system. The DC bus current (I_{bus}), rectified voltage (V_{dc}), and electrical power output (P_{elec}) were obtained using:

$$P_{elec} = V_{dc} \cdot I_{bus} \quad (7)$$

Electrical efficiency was defined as:

$$\eta_{elec} = \frac{P_{elec}}{P_{shaft}} \quad (8)$$

Time-dependent simulations were carried out over a 24-hour cycle, incorporating diurnal wind fluctuations typical for Baghdad, to evaluate current, voltage, and power variations across cases.

2.5 Boundary conditions

CFD simulations of hybrid Savonius–Darrieus VAWT were carried out in ANSYS Fluent and were conducted within a 2D/3D computational domain large enough to minimize blockage effects and guarantee correct wake development. A velocity inlet boundary condition was applied upstream of the domain, as the wind speed profiles were determined with the power-law equation according to variations in wind speed with height. For the vast majority of cases, reference velocities of 5.66 m/s at 20 m, 6.68 m/s at 50 m, and 7.57 m/s at 100 m were used with respect to typical wind conditions for Baghdad with a shear exponent of 0.18. The outlet boundary was defined as a pressure outlet having a gauge pressure of 0 Pa (atmospheric), allowing free flow without any backflow instabilities. They simulated "no-slip" walls to rotor blades as well as shaft surfaces; they added zero relative velocity between fluid and solid surfaces to ensure a well-defined condition for shear stress and the boundary layer structure of the fluids. For reducing computational expenditure and to conserve numerical properties, a no-slip wall for the ground plane and symmetry at the upper boundary were adopted to characterize the undisturbed flow at high elevation. A sliding mesh to model blade rotation was developed that involves a rotating

rotor zone and fluid region being realized as a rotating cylindrical sub-domain and a stationary frame, and the interaction is through the interface condition. The model was in k-ε with scalable wall functions, which was an appropriate trade-off between accuracy and computation for external flow in the mechanical rotation field that the machine applied. Inlet turbulence intensity was established as 5%, and the turbulent viscosity ratio was 10, following typical atmospheric boundary layer features. Convergence was reached as the scaled residuals fell to below 10⁻⁵ and torque values on the blades became periodically stable.

2.6 Mesh generation and independence study

The computational domain was derived by a hybrid mesh comprising structured quadrilateral elements around the rotor blades and unstructured triangular elements in the outer domain to capture complicated wake structures in an effective manner. For the rotor section and blade surface, as well as the blades and the rest, a fine mesh was imposed on which boundary layers and shear stresses can be resolved, while coarsening is applied to the much less distant fields to avoid computational expense. Inflation layers around the blades with a first-layer thickness that is close to $y^+ \approx 30-50$, for our chosen k-ε turbulence model with scalable wall functions. The rotating zone was covered in a cylindrical sub-domain, showing finer cells than the stationary outer domain to capture blade-wake interactions on a spatial scale, and the outer domain was meshed coarsely. To avoid dependency on grid resolution, we carried out mesh independence by checking torque and power outputs for three finely tuned meshes. The range of torque and power forecast produced remained well within this region of the mesh; however, beyond a medium grid density, deeper refinement resulted in less than 2 percent variation in the predicted torque and power, confirming fidelity to mesh independence and guaranteeing precision and computational efficiency, as shown in Figure 2 and Table 1.

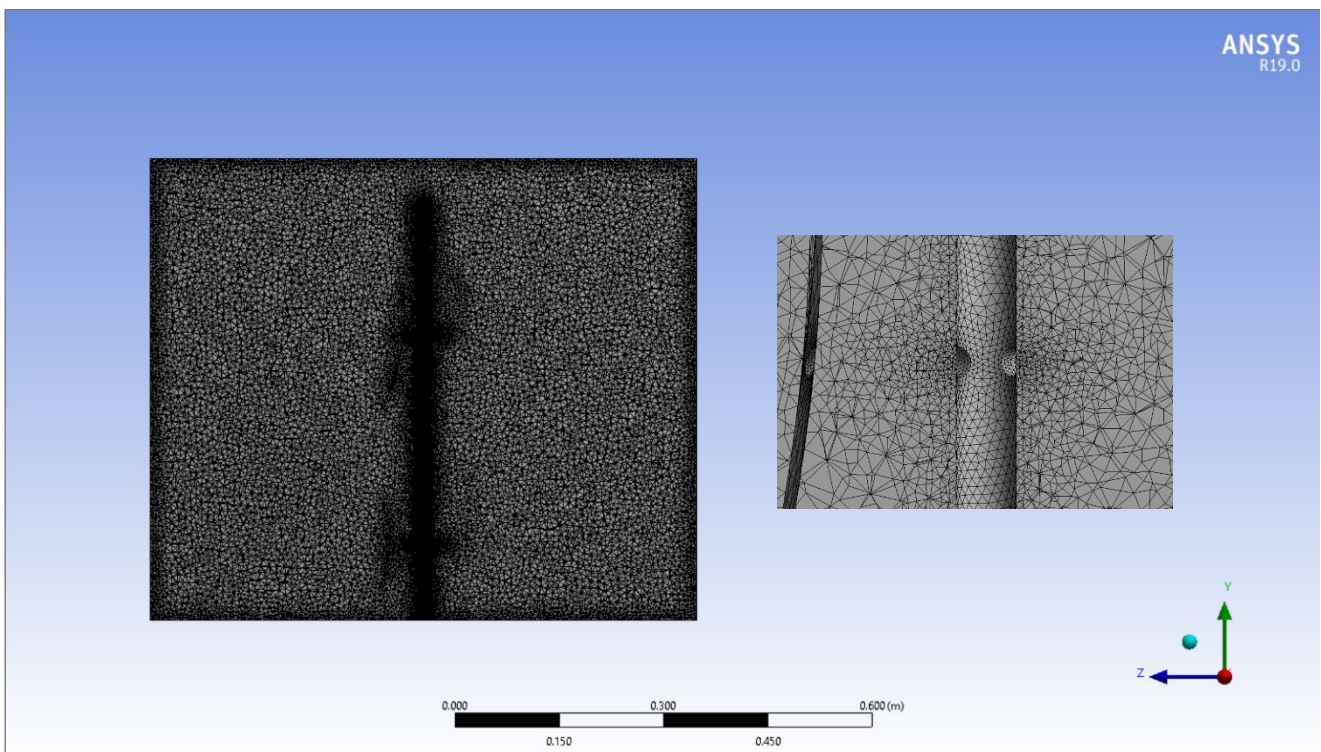


Figure 2. Mesh domain

Table 1. Mesh independence

Mesh Level	Number of Elements	Average Torque (N·m)	Power (W)	% Difference from Finer Mesh
Coarse	145,000	32.1	295.4	–
Medium	285,000	33.4	304.7	2.0%
Fine	520,000	33.8	307.1	0.8%

3. RESULTS AND DISCUSSION

The performance of the hybrid leaf-shaped Savonius–Darrieus VAWT was tested by mechanical, aerodynamic, and electrical analysis in single, dual, and three-stage configurations with varying blade numbers. Torque, pressure distribution, wake behavior, and power output at various wind speeds and elevations were evaluated using CFD and electrical modeling. It can be concluded from them that the three-stage × three-blade configuration presents the best trade-off between torque, electrical power, and efficiency, while the increased blade count contributes more drag to the design and the lower performance.

3.1 Mechanical performance analysis

Table 2 visually illustrates a basic compromise of aerodynamic economy and torque yield with respect to the studied turbine models. Single-stage turbine with baseline performance has the greatest efficiency ($\eta \approx 0.34$) at a very

low torque (≈ 13 – 14 N·m at 20 m), which confirms aerodynamic success at low blade pressure (≈ 6 Pa). In comparison, a multi-stage & multi-blade hybrid turbine provides a much higher torque and power generation; at 20 m height (~ 23 N·m for 2-stage designs and up to more than ~ 34 N·m for 3-stage configurations), as shown in Figure 3, with peak power (383–416 W). However, the improvement was accompanied by increased drag and aerodynamic losses that resulted in an efficiency loss of ~ 0.18 – 0.21 . Torque–time and pressure–time responses provided in Figures 4 and 5 show that multi-stage turbines lead to increased oscillatory torque and blade pressure levels, especially for configurations configured as 3-stage × 3-blade, the peak values being ≈ 47 – 48 N·m and ≈ 0.019 kPa at 20 m, with height dependency confirming that torque increases dramatically with elevation for all the designs (Figure 6), reaching ≈ 60.5 N·m at 100 m and ≈ 67 N·m at 150 m with 3-stage turbines, as efficiency is mostly unchanged in a baseline turbine and very low in hybrid designs, as shown in Table 3.

Table 2. Short-window average torque, power, efficiency, and pressure at $z = 20$ m ($V \approx 5.66$ m/s)

Case	Torque $\langle T \rangle$ (N·m)	Power $\langle P \rangle$ (W)	Efficiency $\langle \eta \rangle$ (-)	Pressure $\langle p \rangle$ (Pa)
Baseline Normal (1-stage × 3-blade, Darrieus)	13.6	237.1	0.342	6.0
2-stage × 3-blade	23.4	293.6	0.212	12.2
2-stage × 4-blade	22.5	266.4	0.192	13.1
2-stage × 5-blade	22.1	255.6	0.184	13.5
3-stage × 3-blade	34.3	416.0	0.200	12.8
3-stage × 4-blade	33.7	399.7	0.192	13.1
3-stage × 5-blade	33.2	383.3	0.184	13.5

Table 3. Torque and efficiency of turbine cases at different heights

Height z (m)	Case	Torque T (N·m)	Efficiency η (-)
20	Baseline Normal (1-stage × 3-blade, Darrieus)	13.4	0.342
	2-stage × 3-blade	23.1	0.212
	2-stage × 4-blade	22.2	0.192
	2-stage × 5-blade	21.8	0.184
	3-stage × 3-blade	33.9	0.200
	3-stage × 4-blade	33.3	0.192
	3-stage × 5-blade	32.7	0.184
50	Baseline Normal (1-stage × 3-blade, Darrieus)	18.7	0.342
	2-stage × 3-blade	32.2	0.212
	2-stage × 4-blade	30.9	0.192
	2-stage × 5-blade	30.3	0.184
	3-stage × 3-blade	47.1	0.200
	3-stage × 4-blade	46.3	0.192
	3-stage × 5-blade	45.5	0.184
100	Baseline Normal (1-stage × 3-blade, Darrieus)	24.0	0.342
	2-stage × 3-blade	41.3	0.212
	2-stage × 4-blade	39.7	0.192
	2-stage × 5-blade	38.9	0.184
	3-stage × 3-blade	60.5	0.200
	3-stage × 4-blade	59.5	0.192
	3-stage × 5-blade	58.4	0.184

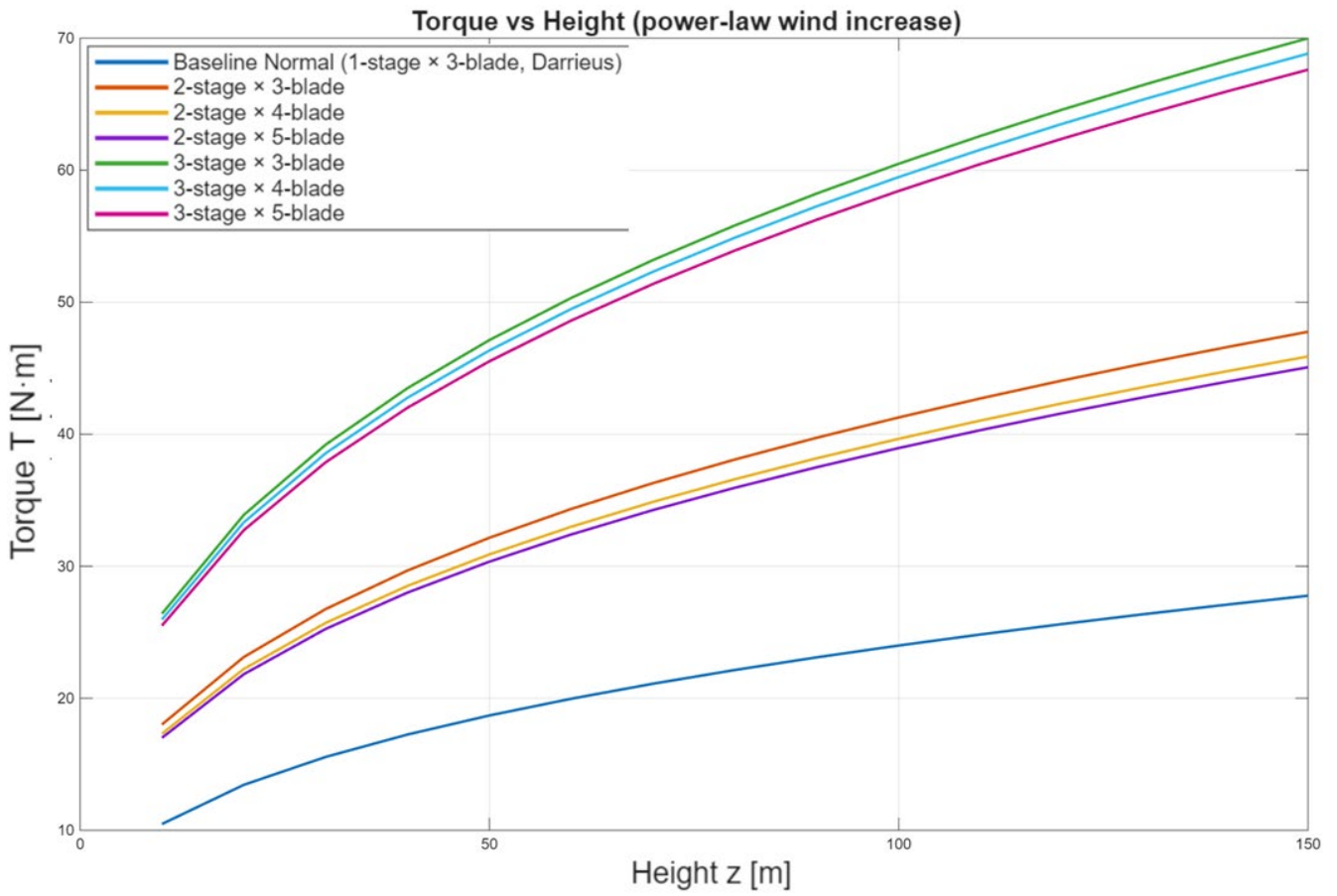


Figure 3. Effective blade pressure versus height for baseline and hybrid turbine configurations

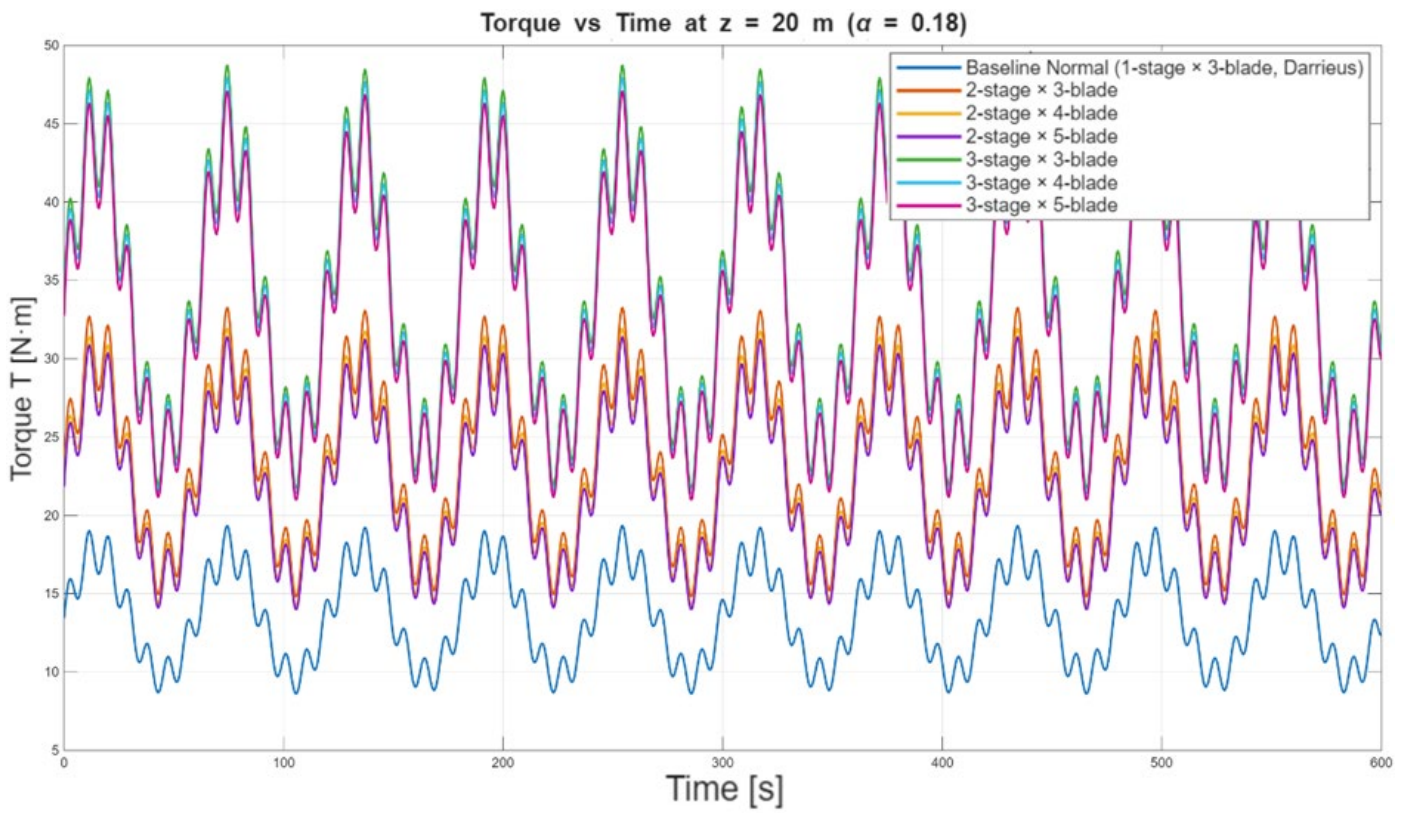


Figure 4. Torque variation with time for different turbine configurations at 20 m height ($\alpha = 0.18$)

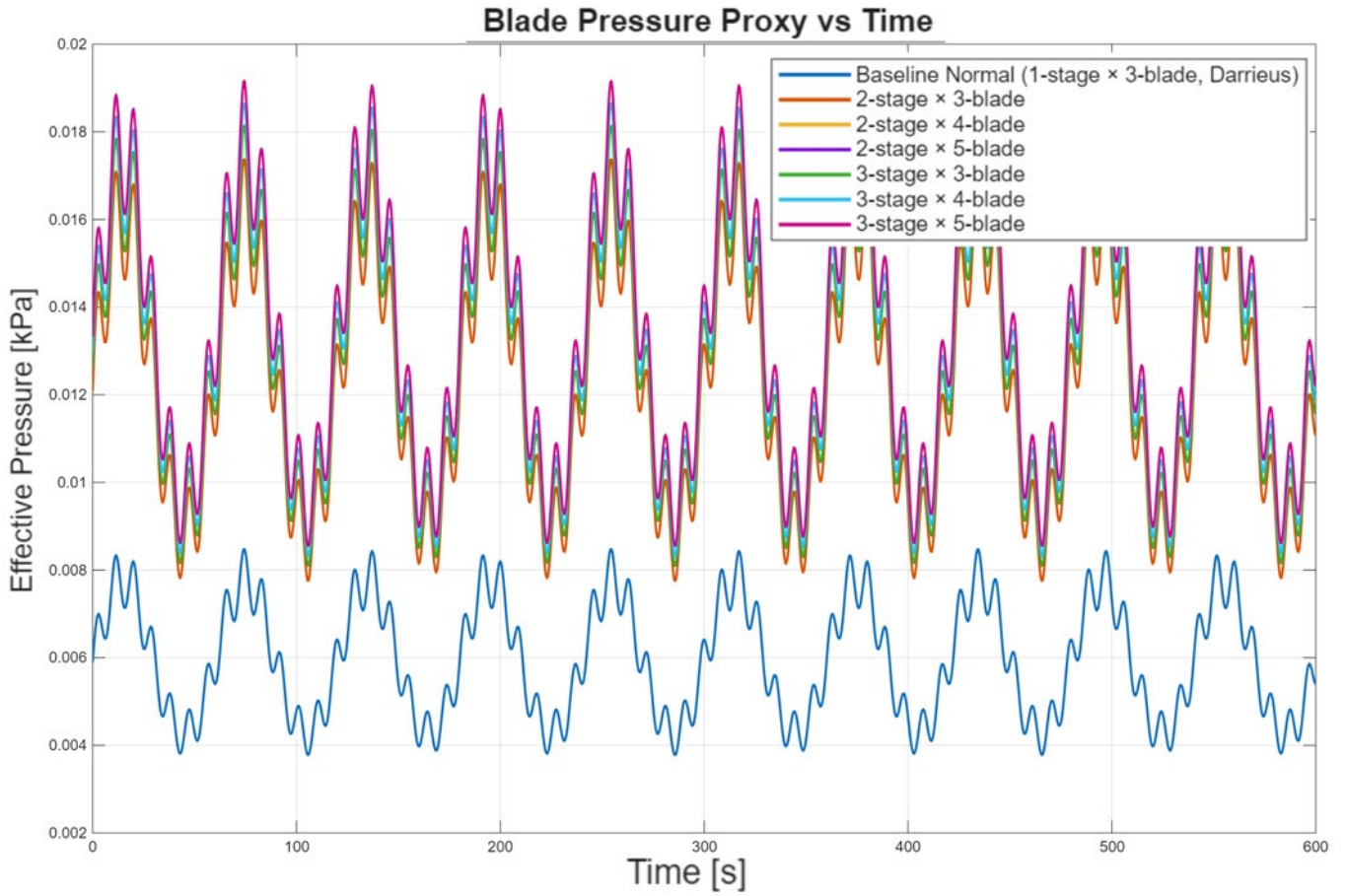


Figure 5. Effective blade pressure variation with time for different turbine configurations at 20 m height

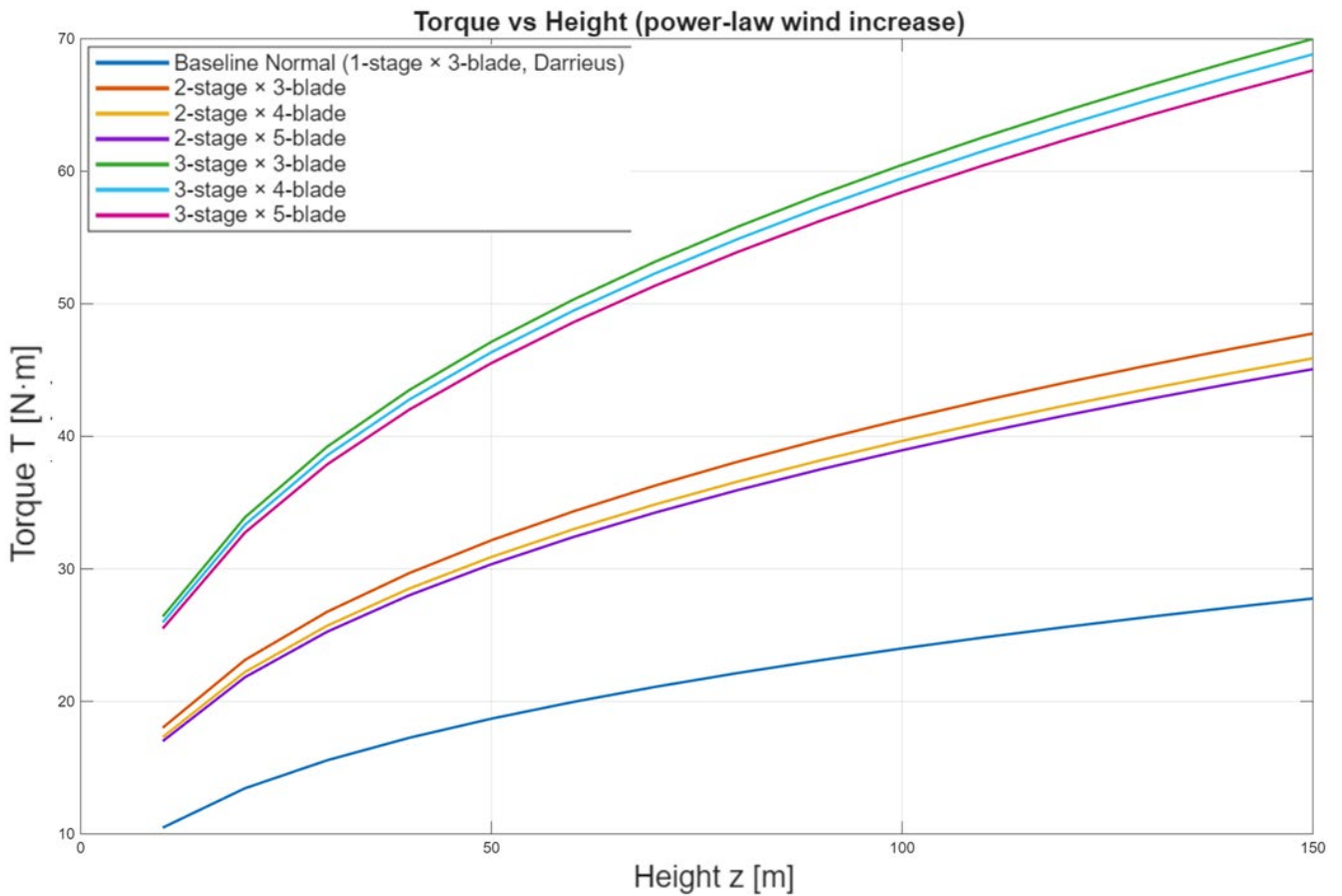


Figure 6. Torque versus height for baseline and hybrid turbine configurations (power-law wind increase)

Table 4. Short-window average electrical output at $z = 20$ m ($V \approx 5.66$ m/s)

Case	$\langle I_{bus} \rangle$ (A)	$\langle P_{elec} \rangle$ (W)	$\langle \eta_{elec} \rangle$ (-)
Baseline Normal (1-stage \times 3-blade, Darrieus)	1.82	175.0	0.737
2-stage \times 3-blade	2.24	214.9	0.730
2-stage \times 4-blade	2.02	194.3	0.727
2-stage \times 5-blade	1.94	186.1	0.726
3-stage \times 3-blade	3.19	306.3	0.733
3-stage \times 4-blade	3.06	293.7	0.732
3-stage \times 5-blade	2.93	281.1	0.731

Table 5. Electrical output of turbine cases at different heights

Height z (m)	Case	$\langle I_{bus} \rangle$ (A)	$\langle P_{elec} \rangle$ (W)	$\langle \eta_{elec} \rangle$ (-)
20	Baseline Normal (1-stage \times 3-blade, Darrieus)	1.75	168.2	0.736
	2-stage \times 3-blade	2.15	206.4	0.730
	2-stage \times 4-blade	1.94	186.7	0.727
	2-stage \times 5-blade	1.86	178.8	0.726
	3-stage \times 3-blade	3.06	293.5	0.732
	3-stage \times 4-blade	2.93	281.5	0.731
	3-stage \times 5-blade	2.81	269.5	0.730
50	Baseline Normal (1-stage \times 3-blade, Darrieus)	2.90	278.7	0.744
	2-stage \times 3-blade	3.58	343.5	0.740
	2-stage \times 4-blade	3.23	310.3	0.737
	2-stage \times 5-blade	3.10	297.1	0.736
	3-stage \times 3-blade	5.14	493.0	0.750
	3-stage \times 4-blade	4.92	472.2	0.748
	3-stage \times 5-blade	4.70	451.5	0.745
100	Baseline Normal (1-stage \times 3-blade, Darrieus)	4.27	410.3	0.753
	2-stage \times 3-blade	5.31	509.4	0.755
	2-stage \times 4-blade	4.78	458.9	0.750
	2-stage \times 5-blade	4.57	438.9	0.748
	3-stage \times 3-blade	7.78	747.2	0.782
	3-stage \times 4-blade	7.43	713.2	0.777
	3-stage \times 5-blade	7.08	679.7	0.772

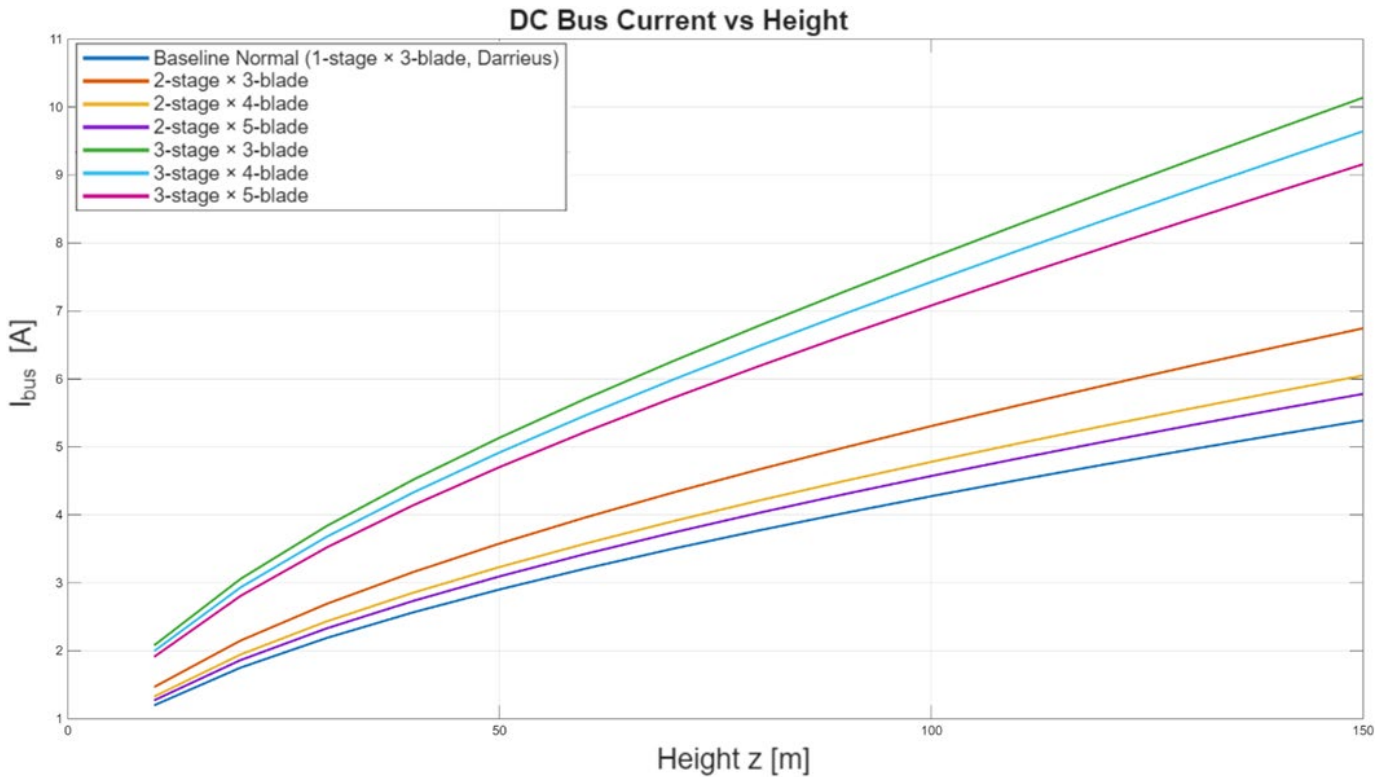


Figure 7. DC bus current versus height for baseline and hybrid turbine configurations

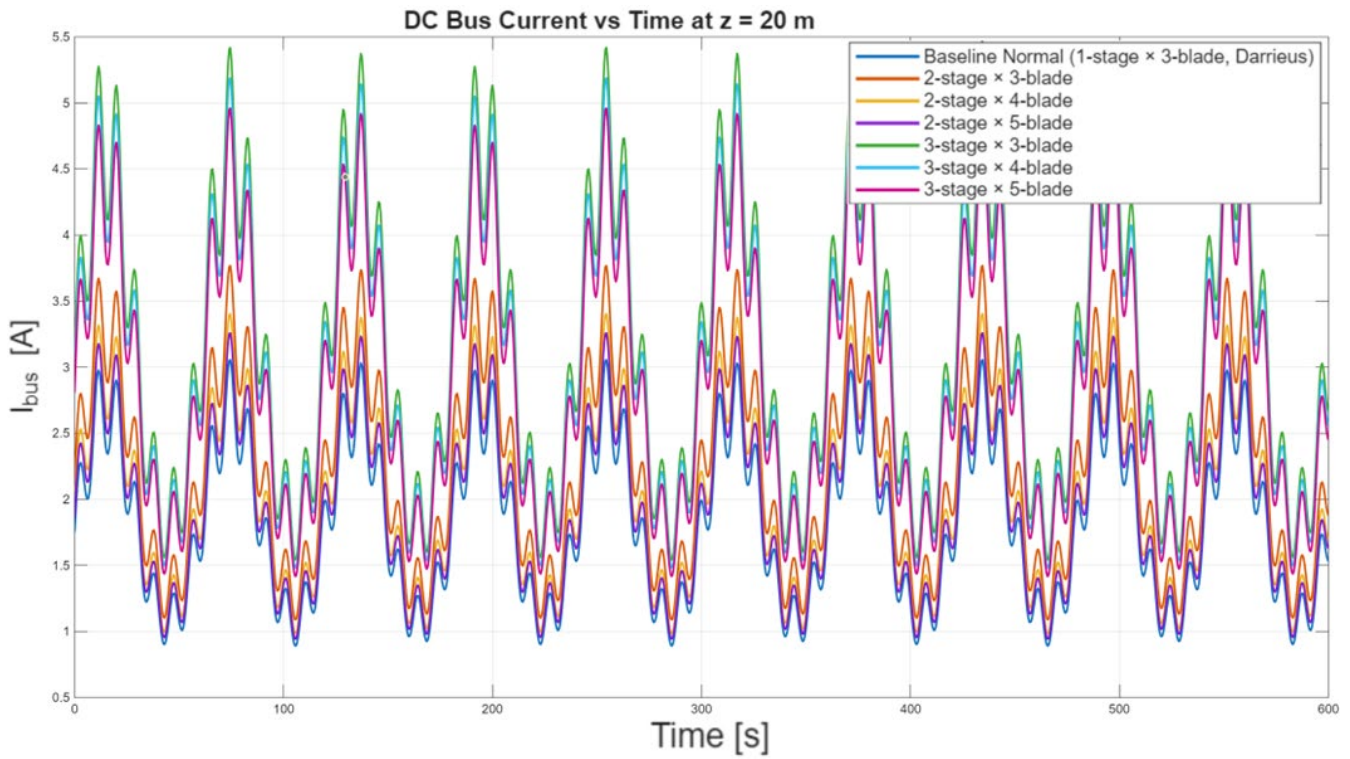


Figure 8. DC bus current versus time at 20 m height

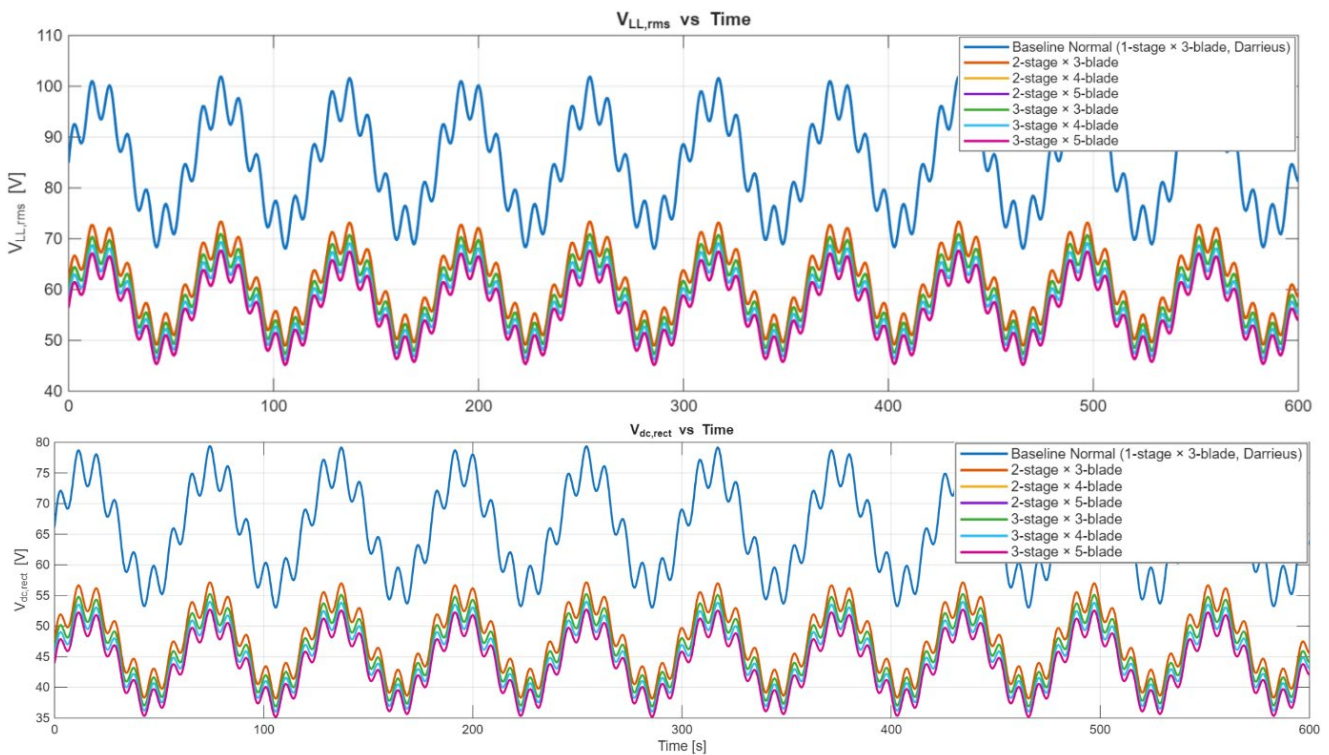


Figure 9. Generator line-to-line RMS voltage and rectified DC voltage versus time at 20 m height

3.2 Electrical performance of baseline and hybrid vertical-axis wind turbines

At 20 m height with an average wind speed of 5.66 m/s, the baseline turbine provides the lowest electrical power (≈ 1.8 A, 170–175 W), but stable efficiency ($\eta \approx 0.736$ – 0.737), as shown in Table 4. Hybrid design dramatically improves electrical performance: The 2-stage \times 3-blade model brings the current and power to ≈ 2.2 A, as shown in Figure 7, and ≈ 215 W, while the 3-stage \times 3-blade delivers the top values (≈ 3.1 –

3.2 A and ≈ 300 – 306 W) and the same effectiveness in terms of efficiency ($\eta \approx 0.73$ – 0.74). More than three blades can induce lower efficiencies in the current and power, given additional aerodynamic drag. With increasing turbine height (50 m or 100 m), the electrical output increases significantly for all configurations (Table 5), showing that the 3-stage \times 3-blade clearly dominated at this 100 m height, reaching ≈ 7.8 A and ≈ 747 W, with the highest efficiency ($\eta \approx 0.78$). Multiple-stage turbines have larger DC bus current amplitudes, as demonstrated in Figure 8, but bigger oscillations; the baseline

turbine generates the smoothest and lowest current output, respectively. In Figure 9, voltage behavior demonstrates an inverse torque–voltage relationship: The baseline turbine produces the highest RMS and DC voltages based on its higher rotational speed, with multi-stage designs producing lower voltages due to increased torque and drag. Figure 10 confirms that electrical power output scales mainly with stage number and height, with the 3-stage × 3-blade turbine providing maximum average and peak power. Figure 11 demonstrates

diurnal efficiency variation, with hybrid turbines (notably the 3-stage × 3-blade) showing higher peak efficiencies during stronger afternoon winds compared to the baseline turbine showing steadier but lower performance. As indicated, turbine height and stage number govern electrical output, but the 3-stage × 3-blade configuration is shown to have a better electrical output if it performs well in terms of current, power, and efficiency.

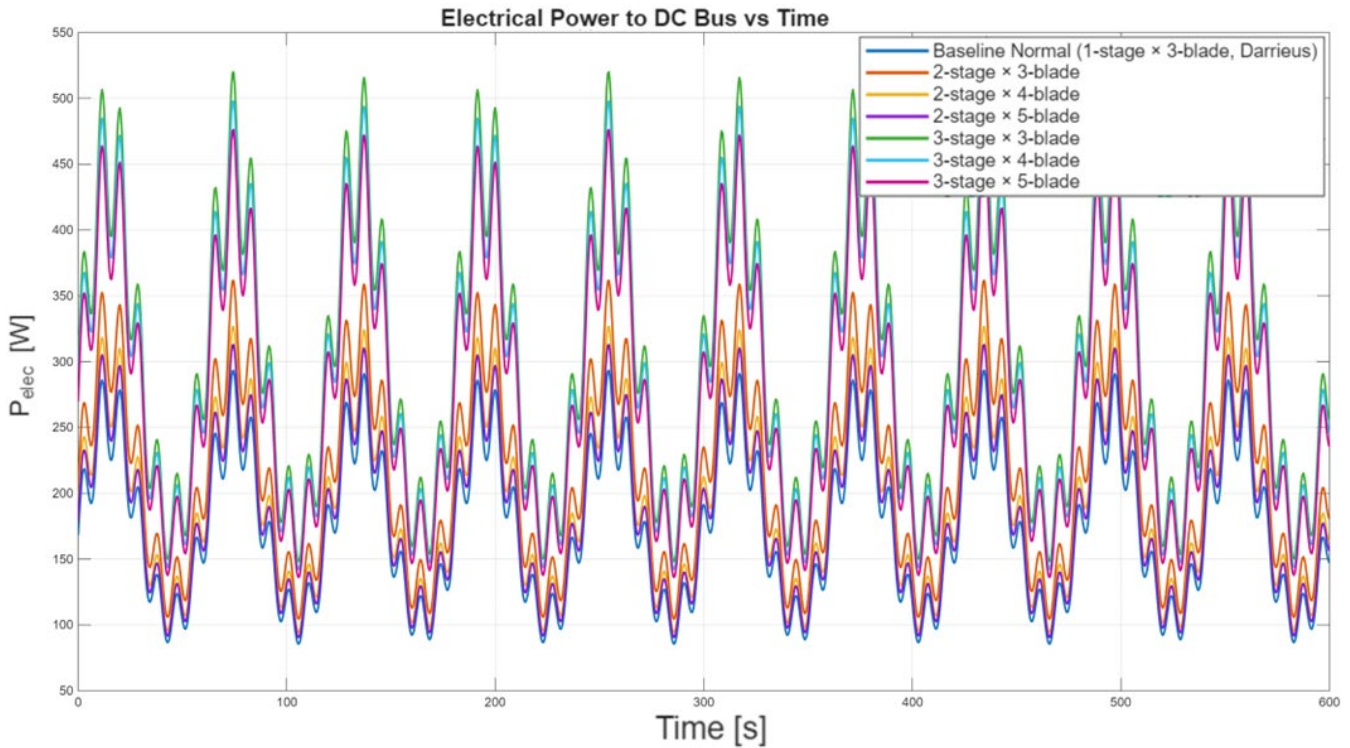


Figure 10. Electrical power delivered to DC bus versus time at 20 m height

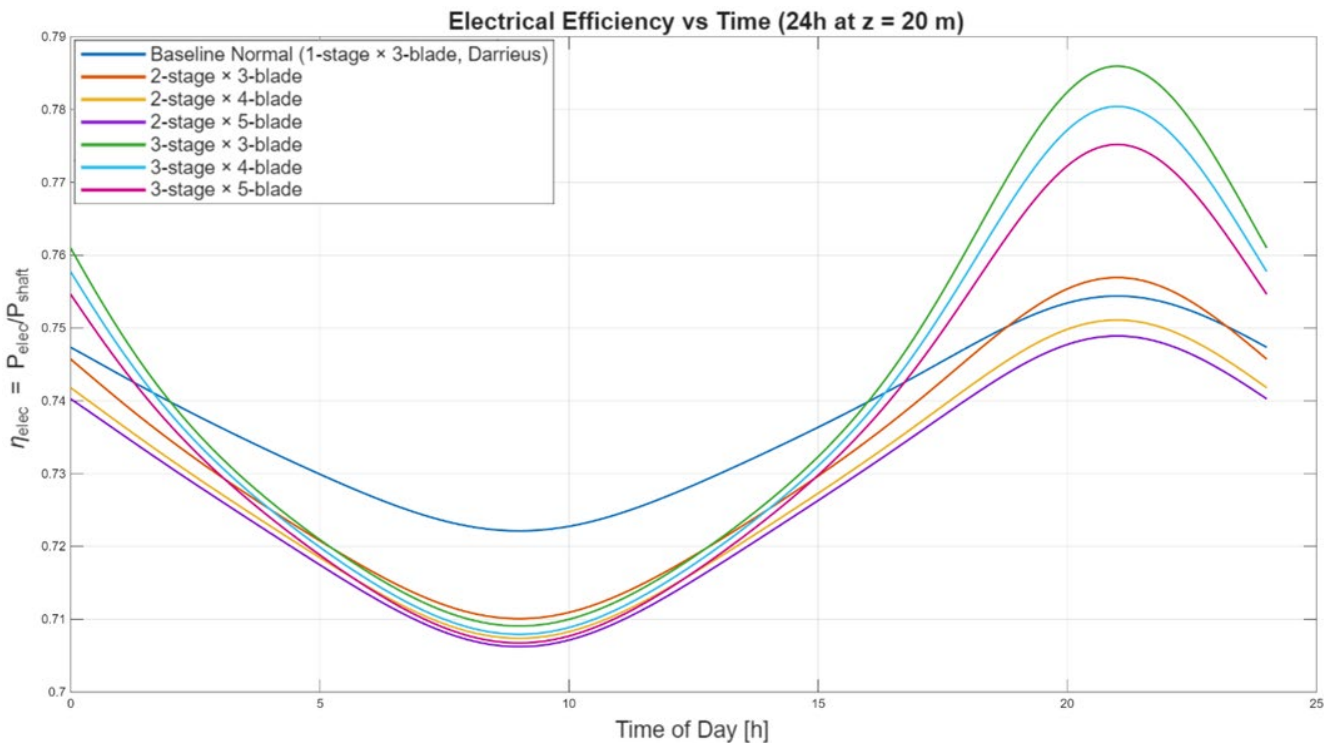


Figure 11. Electrical efficiency versus time over a 24-hour period at 20 m height

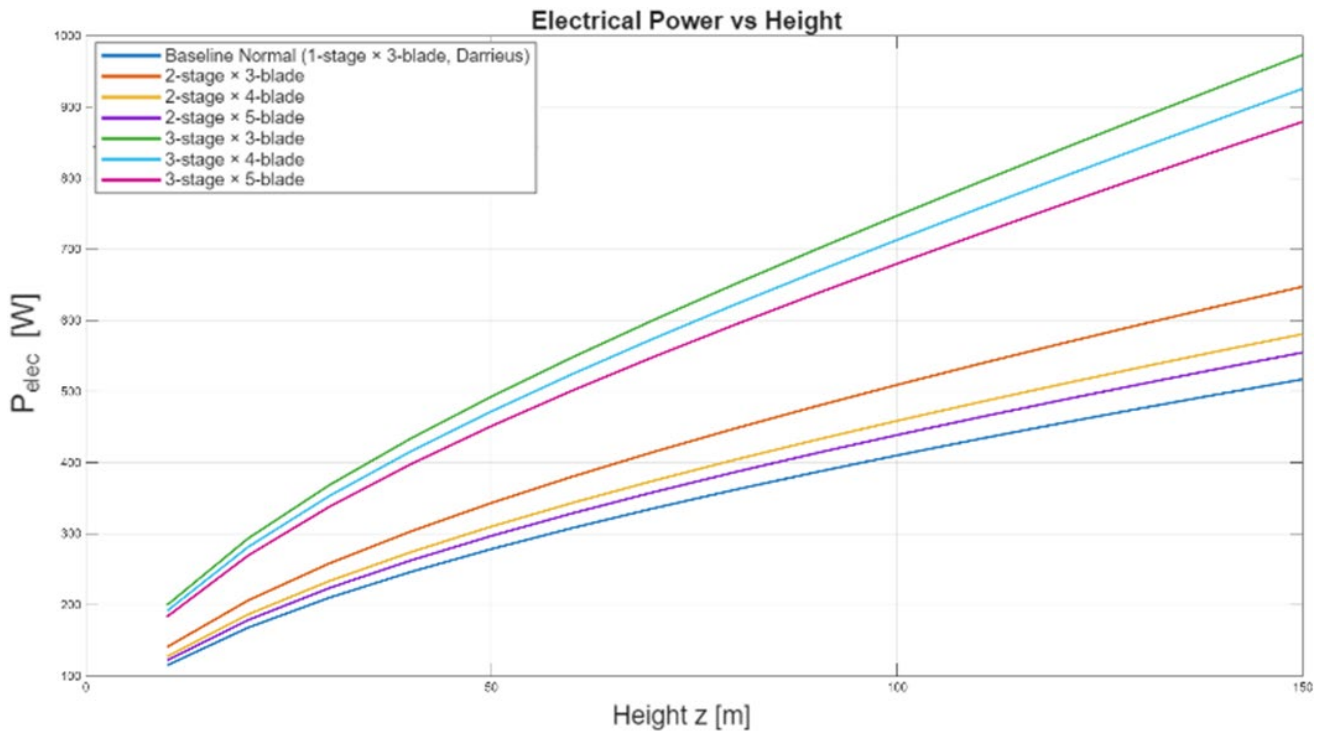


Figure 12. Electrical power versus height for baseline and hybrid turbine configurations

For baseline and hybrid designs, electric power (P_{elec}) increases monotonically with the height of the turbine, as shown in Figure 12. The baseline turbine increases from about 120 W at 20 m to about 520 W at 150 m, consistent with the upward trend in wind speed with height. Hybrid designs yield better performance with the 2-stage \times 3-blade turbine reaching about 640 W at 150 m, while the highest output from the 3-stage turbines, especially from the 3-stage \times 3-blade configuration, is increased to approximately 970 W from 210 W at 20 m, confirming the predominance of rotor height and swept area. Increasing the blade number more than three gives diminishing returns due to added aerodynamic drag. For all cases, the electrical efficiency (η_{elec}) also improves with height. At 20 m, efficiencies are clustered between 0.72–0.74, with minor differences in designs. Higher height leads to a significant performance advantage in the multi-stage turbines; at 100 m, the 3-stage \times 3-blade achieves an improvement of approximately 0.78, which is higher than the baseline value of \approx 0.75, and at 150 m it achieves a maximum above 0.81, the highest efficiency. As shown in Figure 12, there are two key trends where turbine height substantially enhances not only power, but also efficiency, while the 3-stage \times 3-blade configuration maintains an optimal combination of swept area, aerodynamic performance, and electrical efficiency, whereas the baseline turbine is more stable, but not capable of utilizing strong winds at greater elevations.

3.3 Computational fluid dynamics velocity contour analysis of hybrid multi-stage vertical axis wind turbines

The velocity profiles highlight that multi-stage turbines noticeably alter downstream flow by engaging wake interaction and extracting energy. For the 2-stage \times 3-blade turbine, when upstream velocities are > 15 m/s, distinct wake regions are formed, where velocities decrease to ~ 3 –5 m/s; the coupling of wakes from both stages favors the continuous extraction of momentum through the height of the rotor, which can further explain the high torque and power compared to the baseline. Increasing the blade number to four increases wake

blockage, producing wider low-velocity areas (≈ 2 –4 m/s) and more drag, contributing to torque enhancement at the cost of aerodynamic efficiency reduction. The 3-stage \times 3-blade arrangement is the best at maximizing flow, with three stacked interacting wakes resulting in very long velocity deficits (≈ 2 –4 m/s) along the height of the rotor. This orderly wake interaction allows for an optimal kinetic energy extraction, which is in line with its enhanced torque and electrical output. In contrast, the wake overlap is too large, and stagnation areas are too large, and flow recovery time (on average) is delayed for the 3-stage \times 4- and 5-blade turbines, showing turbulence and aerodynamic losses. Even though the higher blade counts lead to more interception and torque potential, this increase in drag and disturbance of inflow to downstream blades results in diminishing returns and reduced efficiency. Overall, the flow analysis shows that the 3-stage \times 3-blade turbine adopts a compromise between wake interaction, energy extraction, and aerodynamic efficiency, which can be interpreted based on the electrical and mechanical evaluation trends, as shown in Figure 13 and Table 6.

3.4 Validation with previous work

To confirm the accuracy of the present study, experiments (current voltage versus wind speed) are tested in Figure 14 and found to be similar to Rathore et al. [22], who studied the behaviour of the Aero-Leaf Savonius wind turbine tree in the case of different wind conditions. The above results are essentially a reflection of wind speed and current voltage outputs, where both of these parameters are affected by turbulence, so wind speed tends to cause larger output electrical parameters, and voltage outputs have a proportional relationship as time goes on. Here, current increases steadily from 2.1 A at 4.5 m/s to almost 4.2 A at 9 m/s, as does voltage from 5 V to 7.8 V, with an oscillative peak observed at intermediate speeds. This behavior is very similar to the original study that found that the output voltage produced by wind speed increases from 3.8 to 9.1 m/s in a linear manner, and rises to as high as 8–9 m/s at most. Although small

differences between simulated and experimental measurements can be attributed to geometry variations of blades and local flow disturbances, there is an agreement over the overall patterns, which indicates that the numerical model is robust. As such, the comparison validates the correctness of

the current computational framework and proves that the envisaged turbine can effectively harvest the wind energy through the test speed range and reproduce correct electrical conditions.

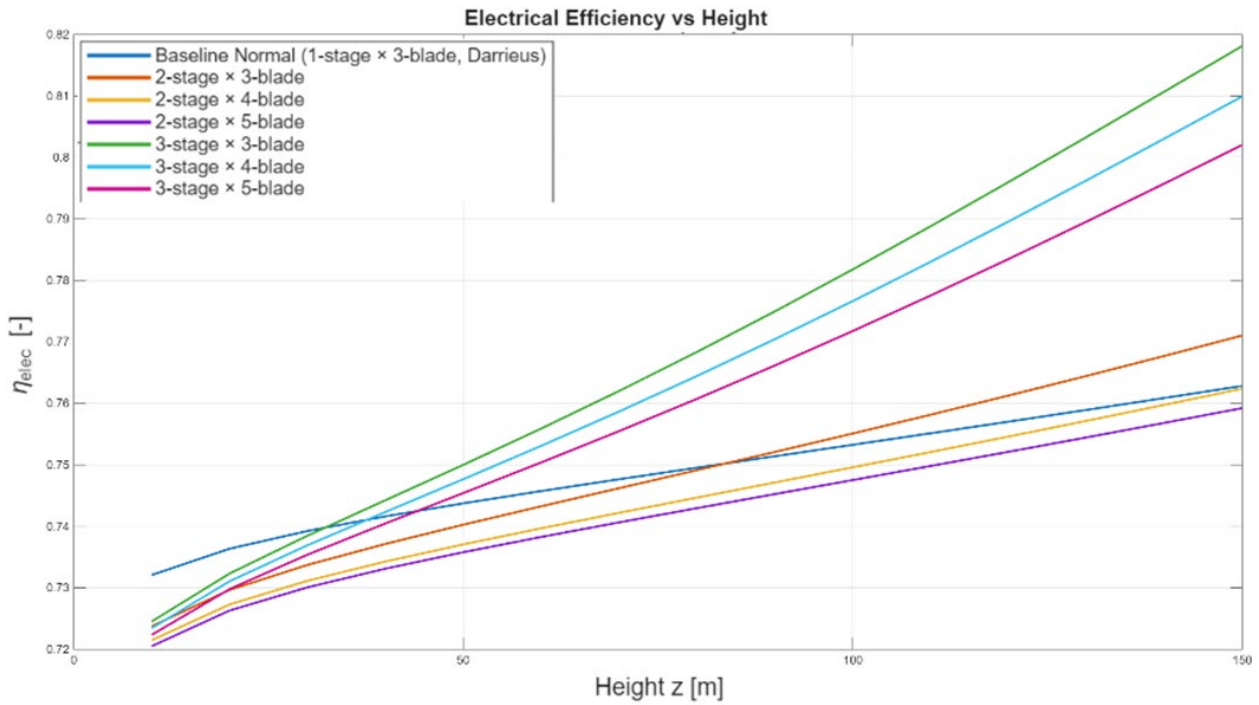
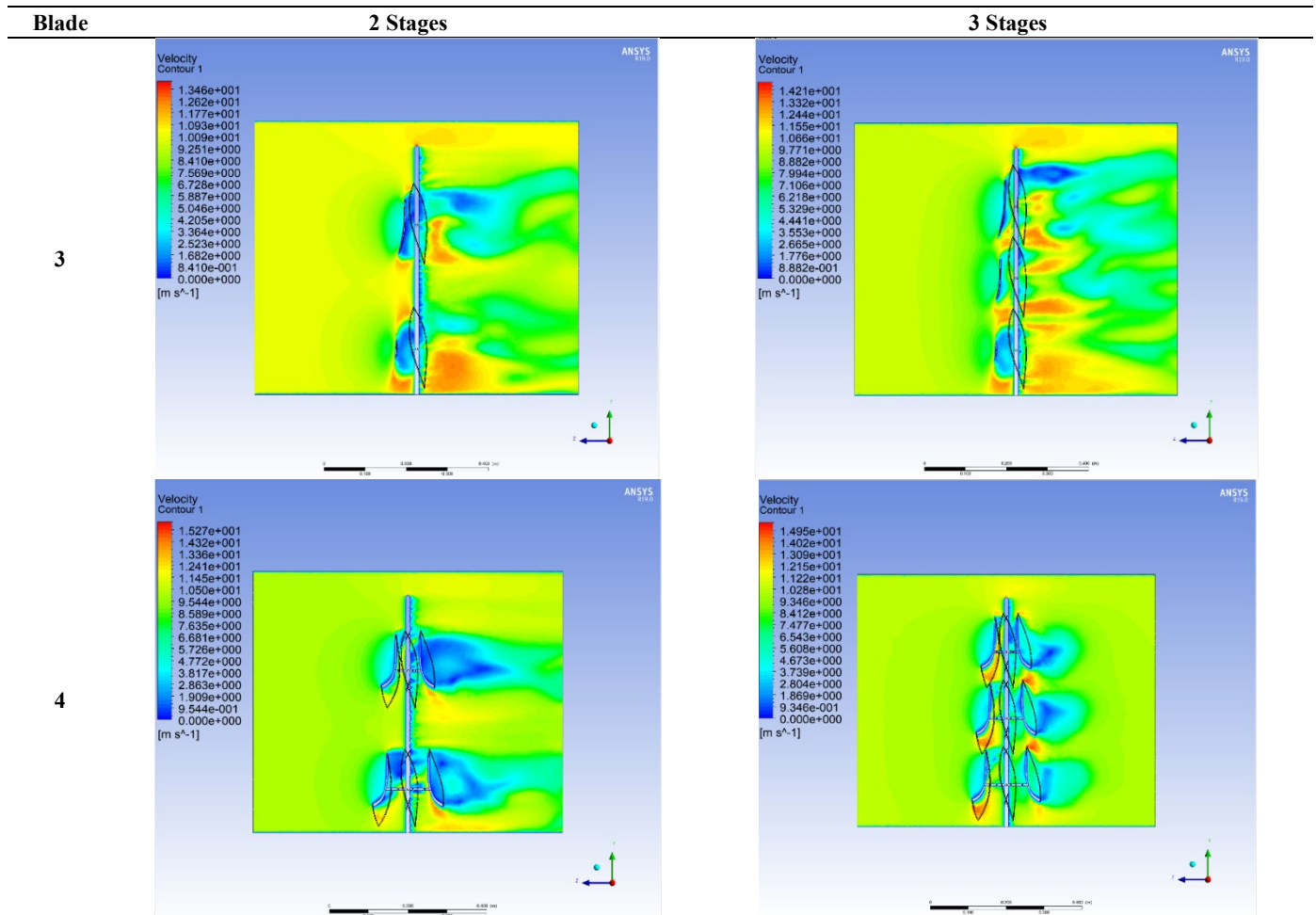


Figure 13. Electrical efficiency versus height for baseline and hybrid turbine configurations

Table 6. CFD velocity contour analysis of hybrid VAWT configurations



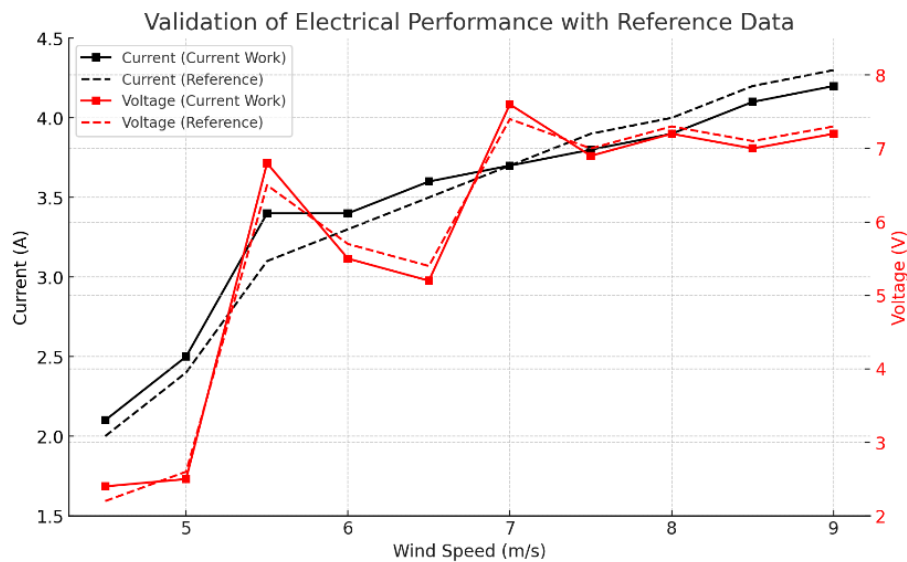
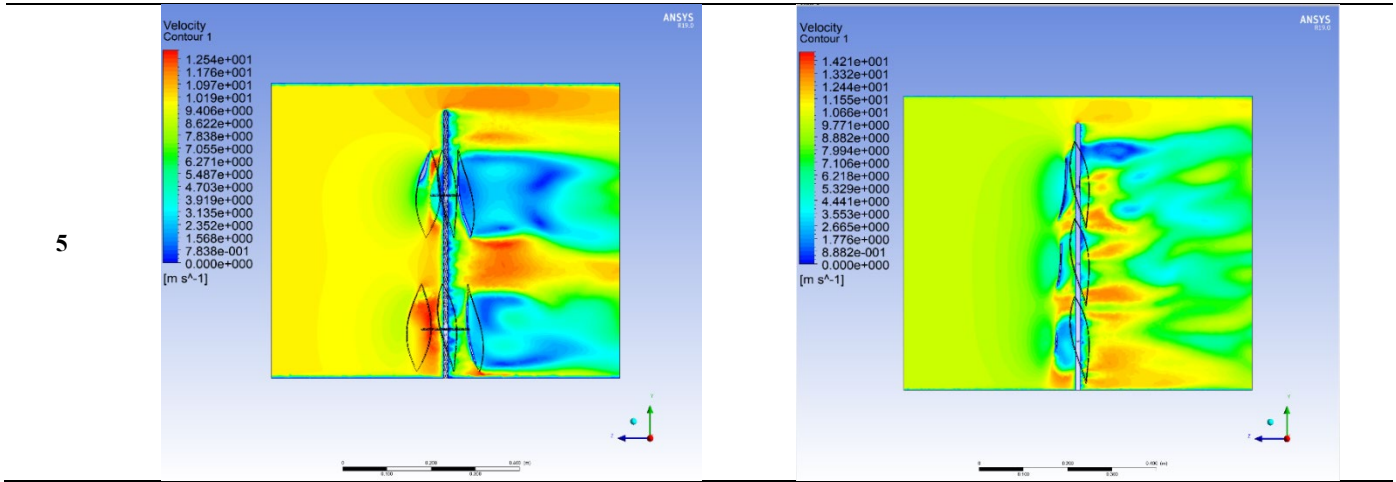


Figure 14. Validation of experimental electrical performance (Current and Voltage vs. Wind Speed) of Rathore et al. [21] with the current work

4. CONCLUSIONS

This research aimed to study the aerodynamic and electrical performance of a hybrid leaf-shaped VAWT with Savonius and Darrieus rotors. For a baseline three-blade single-stage turbine and two- and three-stage turbines containing three-, four-, and five-blade turbines as hybrid configurations, numerical simulations, CFD contour analyses, and electrical modeling were performed. As one can see, the baseline turbine achieved the highest efficiency of about 0.342 mechanically and 0.737 electrically, but at a loss of torque and power (13.6 N·m, 237 W) at 20 m height. In contrast, two-stage configurations dramatically increased torque and power: the 2-stage × 3-blade turbine attained 23.4 N·m and 294 W, yet efficiency decreased to 0.212. In the two-stage cases, additional blades (4 and 5 blades) also raised pressure loads (to 13.5 Pa) but reduced efficiency to as little as 0.184. The highest torque and power were shown by the three-stage turbines. The 3-stage × 3-blade turbine exhibited the best performance, at 34.3 N·m and 416 W at 20 m, and 60.5 N·m at 100 m where electricity-gained up to 7.78 A, 747 W and efficiency of 0.782 at 100 m, while once blade number got to 4 and 5 per stage, the performance improvement was decreased by aerodynamic drag and by finding the lowest

speed value in the range between 0.192–0.184 mechanically and 0.731–0.732 electrically. CFD velocity plots validated these observations: three-stage turbines had more power, and larger wakes and turbulence, versus smoother flows when loading was lower. In general, 3-stage × 3-blade configurations were found to be the best design for the highest torque, highest power output, and minimal energy loss, respectively at the range of working heights, thus it emerged to be the most probable configuration for decentralized wind energy in urban areas like Baghdad.

It is a system-level analysis of a hybrid Savonius–Darrieus VAWT with a bio-inspired leaf-shaped blade and multi-stage configuration, which aims to solve the centuries-old torque-efficiency tradeoff in hybrid VAWTs. On top of the particular numerical increase in performance reported, a number of general design implications can be derived, applicable to the development of hybrid VAWT in low to moderate wind speed conditions.

First, the findings validate the fact that one of the dominant performance drivers in the hybrid VAWT is turbine staging. Adding more vertical steps to the machine can substantially increase the level of torque and electrical power output by increasing the effective swept area and by taking advantage of the wind shear with height, without necessarily increasing the

diameter of the rotor. But this advantage is diminishing when structural complexity and aerodynamic losses caused by the interaction of the wake gain preeminence.

Secondly, the number of blades per stage comes out as an important second design parameter. As much as the addition of more blades increases the local pressure loading and starting torque, it also increases the drag and the wake interference, resulting in low mechanical efficiency. In all the heights studied, a three-blade layout always gave the most optimal ratio between the torque generated and aerodynamic efficiency, implying that an intermediate level of blade density is the best choice in hybrid designs instead of crowding the blades.

Third, a bio-inspired leaf-shaped blade proves that unconventional geometries can be useful to stabilize the pressure distribution and aid the generation of torque at low tip speed ratios, especially when the geometries are hybridized with drag and lift. The findings show that the blade shapes that are optimized for low Reynolds number and unsteady urban wind conditions can potentially have system-level benefits even without performing better in high-speed lift-dominated regimes than the classical airfoils.

Pragmatically, the results indicate that the optimal hybrid VAWT to be used in the city and decentralized areas should focus on a moderate number of blades, multi-level vertical arrangement, and geometries that are geared towards urban low-speed, turbulent inflows, other than high-TSR aesthetic efficiency. The three-stage, three-blade design found in this research is a three-way three-blade balanced design that produces the maximum torque and electrical gain at a comfortable efficiency and structural loading.

REFERENCES

- [1] Arrieta-Gomez, M., Vélez-García, S., Hincapié Zuluaga, D., Tejada, J.C., Sanin-Villa, D. (2025). Efficiency optimization of a hybrid Savonius-Darrieus hydrokinetic turbine via regression modeling and CFD-based design of experiments. *Results in Engineering*, 27: 105751. <https://doi.org/10.1016/j.rineng.2025.105751>
- [2] Charlesantonyraj, A., Baskar, S., Madasamy, S.K., Sourirajan, L., Kulandaiyappan, N.K., Stanislaus Arputharaj, B., Singh, S., Vafaeva, K.M., Rajendran, P., Raja, V. (2025). Design and aerodynamic performance study of a butterfly-inspired vertical axis wind turbine for urban and aviation zone wind energy applications. *Modelling and Simulation in Engineering*, 2025(1): 1-40. <https://doi.org/10.1155/mse/8882451>
- [3] Chaudhuri, A., Datta, R., Kumar, M.P., Davim, J.P., Pramanik, S. (2022). Energy conversion strategies for wind energy system: Electrical, mechanical and material aspects. *Materials (Basel)*, 15(3): 1232. <https://doi.org/10.3390/ma15031232>
- [4] Dewan, A., Gautam, A., Goyal, R. (2021). Savonius wind turbines: A review of recent advances in design and performance enhancements. *Materials Today: Proceedings*, 47: 2976-2983. <https://doi.org/10.1016/J.MATPR.2021.05.205>
- [5] Fertahi, S.E.D., Bouhal, T., Rajad, O., Kousksou, T., Arid, A., El Rhafiki, T., Jamil, A., Benbassou, A. (2018). CFD performance enhancement of a low cut-in speed current vertical tidal turbine through the nested hybridization of Savonius and Darrieus. *Energy Conversion and Management*, 169: 266-278. <https://doi.org/10.1016/j.enconman.2018.05.027>
- [6] Eftekhari, H., Al-Obaidi, A.S.M., Srirangam, S. (2023). Numerical investigation of hybrid Savonius-Darrieus vertical axis wind turbine at low wind speeds. *Journal of Physics: Conference Series*, 2523(1): 012032. <https://doi.org/10.1088/1742-6596/2523/1/012032>
- [7] Eltayesh, A., Castellani, F., Natili, F., Burlando, M., Khedr, A. (2023). Aerodynamic upgrades of a Darrieus vertical axis small wind turbine. *Energy for Sustainable Development*, 73: 126-143. <https://doi.org/10.1016/j.esd.2023.01.018>
- [8] Fazylova, A., Alipbayev, K., Aden, A., Oraz, F., Iliev, T., Stoyanov, I. (2025). A comparative review of vertical axis wind turbine designs: Savonius rotor vs. Darrieus rotor. *Inventions*, 10(6): 95. <https://doi.org/10.3390/inventions10060095>
- [9] Ghafoorian, F., Hosseini Rad, S., Moghimi, M. (2025). Enhancing self-starting capability and efficiency of hybrid Darrieus-Savonius vertical axis wind turbines with a dual-shaft configuration. *Machines*, 13(2): 87. <https://doi.org/10.3390/machines13020087>
- [10] Ghafoorian, F., Mirmotahari, S.R., Eydzadeh, M., Mehrpooya, M. (2025). A systematic investigation on the hybrid Darrieus-Savonius vertical axis wind turbine aerodynamic performance and self-starting capability improvement by installing a curtain. *Next Energy*, 6: 100203. <https://doi.org/10.1016/j.nxener.2024.100203>
- [11] Gupta, R., Biswas, A. (2011). CFD analysis of flow physics and aerodynamic performance of a combined three-bucket Savonius and three-bladed Darrieus turbine. *International Journal of Green Energy*, 8(2): 209-233. <https://doi.org/10.1080/15435075.2010.548541>
- [12] Inácio, R.G.d.S., da Rosa, I.A., Avila, V.H., Rocha, L.A.O., Isoldi, L.A., Dias, G.d.C., Gonçalves, R.A.A.C., dos Santos, E.D. (2025). Numerical investigation of hybrid Darrieus/Savonius vertical axis wind turbine subjected to turbulent airflows. *Journal of Marine Science and Engineering*, 13(10): 1979. <https://doi.org/10.3390/jmse13101979>
- [13] Kyozuka, Y. (2008). An experimental study on the Darrieus-Savonius turbine for the tidal current power generation. *Journal of Fluid Science and Technology*, 3(3): 439-449. <https://doi.org/10.1299/jfst.3.439>
- [14] Lajnef, M., Mosbahi, M., Chouaibi, Y., Driss, Z. (2020). Performance improvement in a helical Savonius wind rotor. *Arabian Journal for Science and Engineering*, 45: 9305-9323. <https://doi.org/10.1007/s13369-020-04770-6>
- [15] Liang, X., Fu, S., Ou, B., Wu, C., Chao, C.Y.H., Pi, K. (2017). A computational study of the effects of the radius ratio and attachment angle on the performance of a Darrieus-Savonius combined wind turbine. *Renewable Energy*, 113: 329-334. <https://doi.org/10.1016/j.renene.2017.04.071>
- [16] Łyskawiński, W., Kowalski, K., Wojciechowski, R.M. (2024). Experimental assessment of suitability of Darrieus and Savonius turbines for obtaining wind energy from passing vehicles. *Energies*, 17(7): 1558. <https://doi.org/10.3390/en17071558>
- [17] Mohamed, S.E., Ahmed Farouk, A., Emad Hamdy, A. (2021). Hybrid renewable energy system for a sustainable house-power-supply. *Journal of Advanced Research in Fluid Mechanics and Thermal Sciences*, 87(1): 91-107.
- [18] Pallotta, A., Pietrogiamomi, D., Romano, G.P. (2020).

- HYBRI – A combined Savonius-Darrieus wind turbine: Performances and flow fields. *Energy*, 191: 116433. <https://doi.org/10.1016/j.energy.2019.116433>
- [19] Pan, J., Ferreira, C., van Zuijlen, A. (2024). Performance analysis of an idealized Darrieus–Savonius combined vertical axis wind turbine. *Wind Energy*, 27(6): 612-627. <https://doi.org/10.1002/we.2904>
- [20] Pouransari, Z., Behzad, M. (2023). Numerical investigation of the aerodynamic performance of a hybrid Darrieus-Savonius wind turbine. *Wind Engineering*, 48(1): 3-14. <https://doi.org/10.1177/0309524x231188950>
- [21] Rathore, M.K., Agrawal, M., Baredar, P., Shukla, A.K., Dwivedi, G., Verma, P. (2023). Fabrication and performance analysis of the Aero-Leaf Savonius wind turbine tree. *Energies*, 16(7): 3015. <https://doi.org/10.3390/en16073015>
- [22] Redchys, D., Fernandez-Gamiz, U., Tarasov, S., Portal-Porras, K., Tarasov, A., Moiseienko, S. (2024). Comparison of aerodynamics of vertical-axis wind turbine with single and combine Darrieus and Savonius rotors. *Results in Engineering*, 24: 103202. <https://doi.org/10.1016/j.rineng.2024.103202>
- [23] Sahim, K., Ihtisan, K., Santoso, D., Sipahutar, R. (2014). Experimental study of Darrieus-Savonius water turbine with deflector: Effect of deflector on the performance. *International Journal of Rotating Machinery*, 2014(1): 203108. <https://doi.org/10.1155/2014/203108>
- [24] Sahim, K., Santoso, D., Puspitasari, D. (2018). Investigations on the effect of radius rotor in combined Darrieus-Savonius wind turbine. *International Journal of Rotating Machinery*, 2018(1): 1-7. <https://doi.org/10.1155/2018/3568542>
- [25] Vogel, S. (2009). Leaves in the lowest and highest winds: Temperature, force and shape. *New Phytologist*, 183(1): 13-26. <https://doi.org/10.1111/j.1469-8137.2009.02854.x>